ARTICLES
PUBLISHED ONLINE: 11 APRIL 2010 | DOI: 10.1038/NMAT2730
nature materials

The thermodynamic origin of hysteresis in insertion batteries

Wolfgang Dreyer[1], Janko Jamnik[2], Clemens Guhlke[1], Robert Huth[1], Jože Moškon[2] and Miran Gaberščček[2,3]*

Lithium batteries are considered the key storage devices for most emerging green technologies such as wind and solar technologies or hybrid and plug-in electric vehicles. Despite the tremendous recent advances in battery research, surprisingly, several fundamental issues of increasing practical importance have not been adequately tackled. One such issue concerns the energy efficiency. Generally, charging of 10^{10}–10^{17} electrode particles constituting a modern battery electrode proceeds at (much) higher voltages than discharging. Most importantly, the hysteresis between the charge and discharge voltage seems not to disappear as the charging/discharging current vanishes. Herein we present, for the first time, a general explanation of the occurrence of inherent hysteretic behaviour in insertion storage systems containing multiple particles. In a broader sense, the model also predicts the existence of apparent equilibria in battery electrodes, the sequential particle-by-particle charging/discharging mechanism and the disappearance of two-phase behaviour at special experimental conditions.

In the past two decades, hundreds of different active materials for potential use in lithium storage electrodes have been proposed. A common feature of all these materials, as well as all previously known storage systems, is a significant voltage hysteresis between the charge and discharge curve obtained during galvanostatic testing. The hysteresis can be decreased by decreasing the rate of charge and discharge, by particle-size minimization, minimization of electrode thickness and so on. This is expected because in all of these cases we decrease the overvoltage, either by decreasing the current density or by decreasing the impedance resulting from charge transport. However, if this impedance were the only source of voltage hysteresis, the gap between the charge and discharge curve should become vanishingly small when the charge/discharge rate (current) is decreased to a sufficiently small value. The experiments do not support such a scenario but rather indicate that there exists a finite voltage gap between the charge and discharge potential curve even as the current tends towards zero. This phenomenon is illustrated in Fig. 1 on the example of three different, arbitrarily selected Li ion systems: the recently discovered Li_2FeSiO_4 cathode material, an anatase TiO_2 electrode material and the classical $LiCoO_2$ cathode material. The principle of determination of a voltage gap between the charge and discharge curve is shown in Fig. 1a. The gap was determined for different charge/discharge rates. The results for several sets of electrodes prepared from each of the three materials are gathered in Fig. 1b–d. In all cases, the extrapolation to zero current ends up in a residual voltage (denoted as 'zero-current gap'); its value extends from a few millivolts ($LiCoO_2$) to several tens of millivolts (Li_2FeSiO_4, TiO_2). Note that in all of these systems the charge and discharge are described by the same reaction—only its direction changes accordingly. This is a very important distinction with respect to certain conversion reactions where the hysteresis is obviously due to different reaction pathways during charge and discharge[1,2]. A similar reason—different reaction pathways—could be the cause of the huge zero-current gap of up to 1,000 mV as observed in the new Li–air battery reversible system[3].

In the following, we focus on the hysteretic behaviour of $LiFePO_4$. There are two reasons for choosing this particular material. First, $LiFePO_4$ has been one of the most studied Li battery materials during the past years, so a lot of useful data on this material needed for understanding the underlying mechanisms have already been gathered. Second, the charge/discharge voltage curves for $LiFePO_4$ are very flat, which allows for more accurate determination of the voltage gap resulting from hysteresis than in most other systems. The flat voltage profile observed in $LiFePO_4$ materials with a particle size between about 50 and 1,000 nm (Fig. 2a) is due to a phase transition[4]. We focus on the hysteresis that occurs within this flat region, as indicated by the dotted rectangle in Fig. 2a. A $LiFePO_4$ electrode was cycled within the rectangular region at a progressively decreasing rate of charge/discharge down to $C/1{,}000$ (0.17 mA g^{-1}). It can be seen from Fig. 2b that the decreasing rate creates a progressively lower voltage gap between the charge and discharge curve. By analogy to Fig. 1b–d, we could now plot the voltage gap as a function of charge/discharge rate. However, to present the phenomenon in a clearer way, here we choose to divide the total gap into two branches that reflect the deviation from the hypothetic equilibrium potential towards more positive or negative values during charge and discharge, respectively. The result is shown in Fig. 2c. In this representation we see even more clearly the existence of a voltage gap of about 20 mV as we approach the zero current. According to conventional understanding, we would expect that at zero current (corresponding to an equilibrium situation) the voltage gap would also tend to zero. Now a fundamental question emerges. Is it possible that in certain battery systems we have several apparent equilibria (that is, the one at 20 mV but also 0 mV and so on) and if yes, why?

To exclude the specific conditions during the experiment in Fig. 2a–c, we carried out another experiment (Fig. 2d). First we charged a preconditioned (previously cycled) $LiFePO_4$ electrode at a 0.1 C rate (17 mA g^{-1}) up to a 60% state of charge, so that the state of the cathode lay within the flat-potential region, that is, within the two-phase regime (specifically, within the rectangle

[1]Weierstrass Institute for Applied Analysis and Stochastics, DE-10117 Berlin, Germany, [2]National Institute of Chemistry, Hajdrihova 19, SI-1000 Ljubljana, Slovenia, [3]Faculty of Chemistry and Chemical Technology, Aškerceva 5, SI-1000 Ljubljana, Slovenia. *e-mail: miran.gaberscek@ki.si.

© 2010 Macmillan Publishers Limited. All rights reserved.

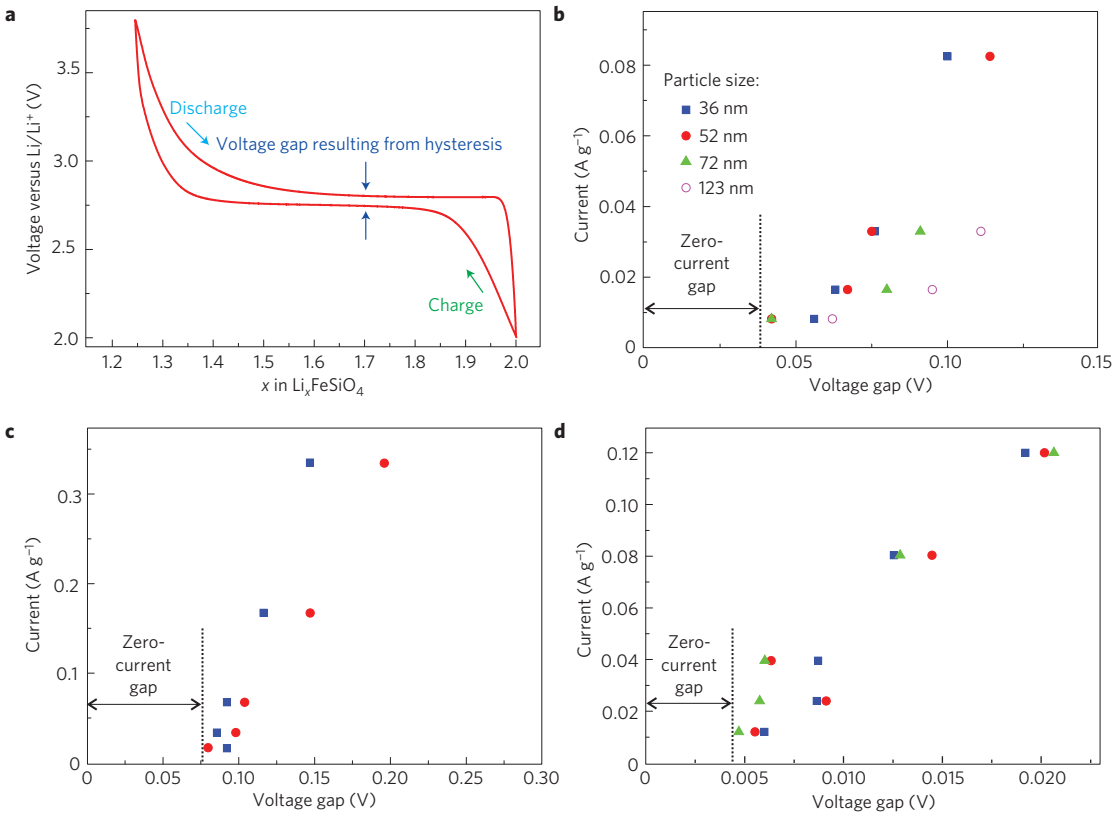

Figure 1 | Demonstration of the existence of a voltage gap at zero current for three different insertion battery materials. a, Definition of a voltage gap on the example of a typical galvanostatic charge/discharge curve for a $LiFePO_4$ material at a rate of $C/20$. **b**, Voltage gap resulting from hysteresis at different charge discharge/currents for several Li_2FeSO_2 electrodes with different mean particle sizes. **c**,**d**, Zero-current voltage gap in two anatase TiO_2 electrodes (**c**) and in several $LiCoO_2$ electrodes (**d**).

in Fig. 2a). After 47 h of rest time, we assumed that the electrode had reached an equilibrium state (Fig. 2d, green point). Then the electrode was discharged within the two-phase region at a very slow rate of $C/1{,}000$ ($0.17\,mA\,g^{-1}$) until a 40% state of charge was reached (Fig. 2d, lower red curve). To allow for a relaxation to an equilibrium, a further rest time of 48 h was applied to reach an open-circuit voltage of 3.418 V (Fig. 2d, blue point at the lower dashed magenta line). Then the electrode was re-charged at a $C/1{,}000$ rate so that the 60% state of charge is reached again (Fig. 2d, upper red curve). After a subsequent rest time of 55 h, the open-circuit voltage was now 3.426 V (Fig. 2d, blue point at the upper magenta dashed line), that is, 8 mV higher than before. It seems that, again, we observe at least two equilibrium potentials.

A third piece of experimental evidence for the existence of two or more apparent equilibrium potentials in $LiFePO_4$ electrodes was based on careful monitoring of open-circuit voltages (apparent equilibrium potentials) of many $LiFePO_4$ cells as a function of cell history. The results are shown in Supplementary Information S1.

The existence of several apparent equilibrium potentials in a system with a symmetrical charge/discharge reaction is highly surprising and requires a deeper explanation. We show that the hysteretic behaviour presented in Figs 1 and 2c is due to the fact that in a battery we have many individual particles that are connected to each other so that fast exchange of lithium between the particles is possible[5]. Furthermore, such interconnected many-particle systems can give rise to many other phenomena that have been observed by other authors in Li insertion systems but have not been properly explained. Examples of such phenomena are discussed in the last part of this article.

To understand the behaviour of a multiparticle ensemble, it is instructive to first look at the properties of a single particle. For simplicity, let us take a single particle of $LiFePO_4$ with a typical dimension in the range from 50 to 1,000 nm and, for a while, neglect the possible mechanical phenomena. Initially, the particle is fully discharged (Li_1FePO_4). The possible shapes of the chemical potential of the Li component as a function of particle composition for various cases are shown in Fig. 3a. The blue non-monotone curve is closely related to the derivative of the bulk free-energy density over the particle composition assuming that the particle is homogeneous[6] (for details see Supplementary Information S2). The solid black line represents the equilibrium potential of the Li component when the particle contains two coexisting phases. Finally, the red part indicates the slightly changed potential path expected in a galvanostatic experiment that, contrary to the widespread belief, is not necessarily an equilibrium experiment, even if the rate is very slow (see also Supplementary Information S2). Thus, during galvanostatic charging, the potential passes the dotted equilibrium line and climbs to the top of the first maximum where the so-called spinodal region is entered. Here two phases are formed inside the particle, one with a high (β) and the other with a low (α) Li mole fraction[4]. During this phase formation, the potential is relaxed to the black dotted horizontal equilibrium line in the $\mu(y)$ plot and the Li mole fractions of the phases can be calculated by means of the classical Maxwell area rule. If the total Li mole fraction of the particle is kept fixed (for example, frozen at a certain point in the typical galvanostatic experiment), this two-phase system is stable. A more detailed single-particle treatment is given in Supplementary Information S2.

If realistic mechanical phenomena (volume change of 6%, existence of surface tension and so on) are taken into account, the Maxwell area rule and thus the position of equilibrium

© 2010 Macmillan Publishers Limited. All rights reserved.

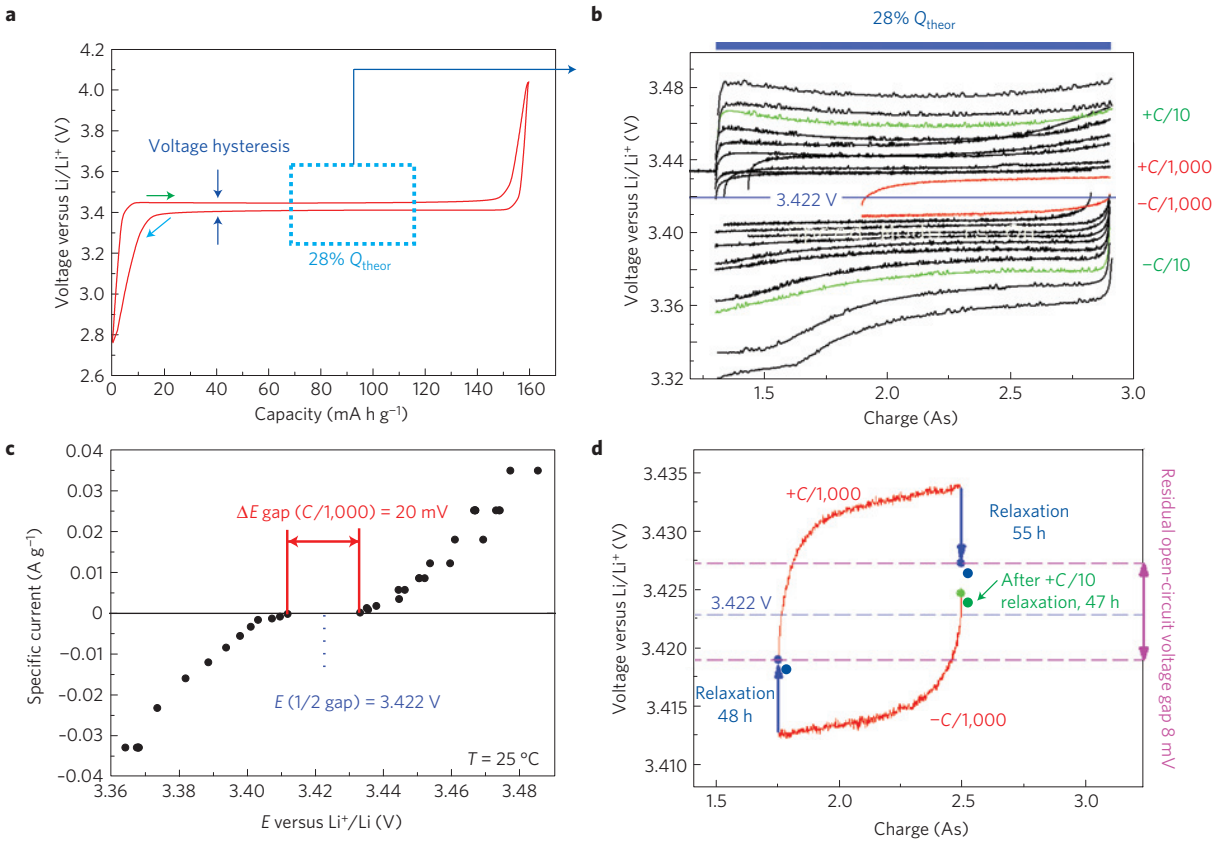

Figure 2 | Precise experiments showing the existence of a zero-current voltage gap in $LiFePO_4$. a, Typical galvanostatic charge/discharge profile for a $LiFePO_4$ electrode at a low rate (*C*/20). The blue rectangle indicates the region that was used for the cycling experiment in **b**. **b**, Galvanostatic charge/discharge profiles for a $LiFePO_4$ electrode at selected rates in the range from *C*/10 to *C*/1,000. **c**, A current–potential plot generated from **b** whereby the points were read from the middle of graph **b**. **d**, Very slow charge/discharge experiment on $LiFePO_4$ with long periods of rest time with the aim to approach the equilibrium behaviour within the plateau region. Details are given in the main text.

changes but all the main one-particle properties remain similar to those indicated in Fig. 3a.

Now we move from the one-particle treatment to an ensemble of many storage particles that can interchange their Li content through interparticle pathways. This exchange is assumed to be fast, so 'communication' between the particles is not hindered during the experiment. The possible mechanical phenomena are also taken into account. We start with a system of homogeneous, fully discharged storage particles (composition Li_1FePO_4). The charge rate is assumed to be much smaller than the diffusional relaxation rate within the particles (the latter is merely a few seconds, if the chemical diffusion coefficient of Li is assumed to be $\leq 10^{-12}$ cm^2 s^{-1} and the particle size is $\leq$50 nm; refs 7, 8). Let the Li mole fraction be gradually decreased so that point A in Fig. 4a is reached where we have a Li-rich solid solution. Then we proceed to point B (corresponding to the maximum in Fig. 3a). At this point, one, two or several particles will become inhomogeneous by forming the two-phase system whereas most will still be in the homogeneous Li-rich solid solution state (β) (see Fig. 4a,b). Now a crucial dilemma arises. Will the two-phase particles be stable (Scenario 1 in Fig. 4b) or will they relax by exchanging lithium with other particles and assume a one-phase state, in this case the α state (see Scenario 2 in Fig. 4b)?

Let us index the particles in a many-particle storage system by $l \in \{1, 2, \ldots, N\}$. The thermodynamic state of a particle l is assumed to be homogeneous and characterized by the Li mole fraction y^l, its mass density ρ^l and its volume V^l.

The total free energy of the considered system is represented by the sum of the individual free energies plus the outer pressure times the total volume of the N storage particles.

$$A = \sum_{l=1}^{N} V^l \left(\rho^l \psi^l + p_0\right) \tag{1}$$

where ψ^l is the specific free energy of particle l. The corresponding chemical potential is defined by

$$\mu^l = m\left(y^l\right) \frac{\partial \psi^l}{\partial y^l} \tag{2}$$

where $m(y^l) = m_{FePO_4} + m_{Li} y^l$ and m_{FePO_4}, m_{Li} denote the molecular weights. We refer again to Fig. 3a, which illustrates the non-monotonicity of the chemical potential (blue and red curves). Note that here we use the same non-monotonic chemical potential as in ref. 6.

The state of charge of the battery is proportional to $(1-q)$, where q is the total Li mole fraction of the many-particle system and it is defined by

$$q = \frac{1}{N} \sum_{l=1}^{N} y^l \tag{3}$$

This constraint tells us that in a many-particle system we can control only the total amount of lithium in all particles, whereas the amount inside individual particles is not known (contrary to established model assumptions[9,10]).

To obtain the necessary conditions for equilibria we determine the minima of the total free energy (1) for a fixed total Li mole

© 2010 Macmillan Publishers Limited. All rights reserved.

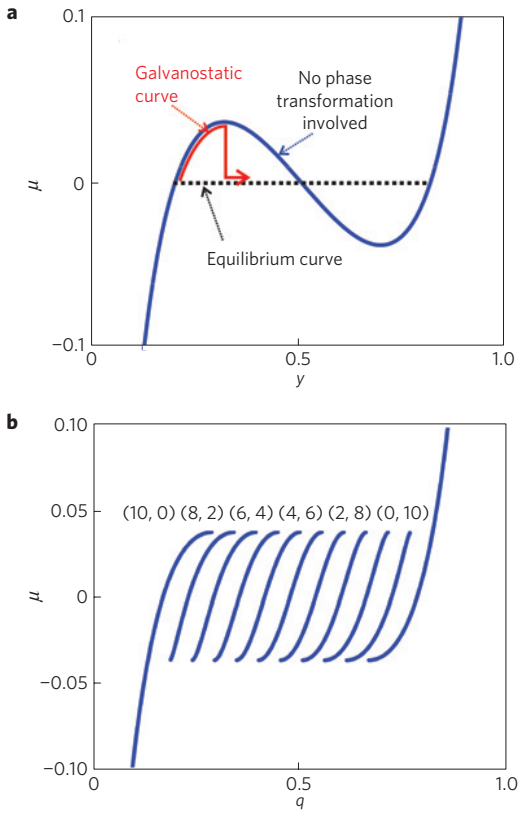

Figure 3 | Comparison of chemical potential profiles in a single-particle and in a 10-particle system. a, Chemical potential profiles for the Li component in a single storage particle showing a positive heat of solution for different cases. The blue non-monotone curve assumes no phase transition. The black line describes a two-phase equilibrium potential. The red path is expected in the case of phase separation controlled by a typical galvanostatic experiment. **b**, Separation of equilibria into different branches of a 10-particle system in the (μ, q) plot.

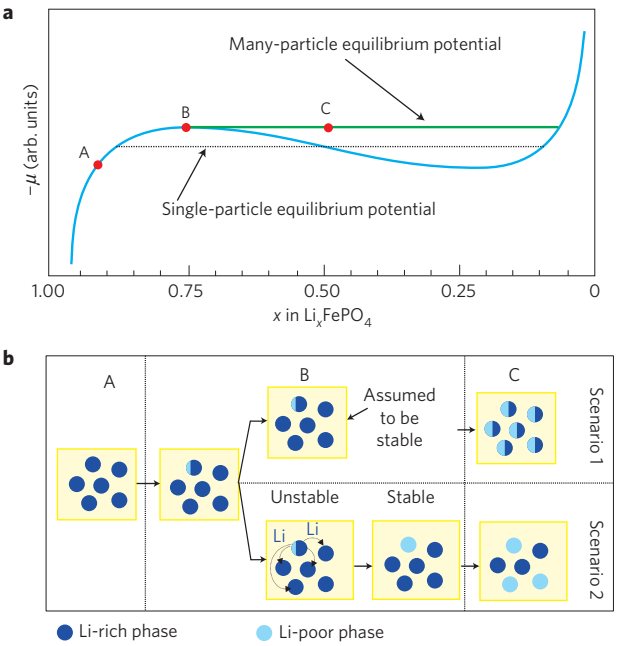

Figure 4 | Two possible scenarios of new phase formation in a many-particle system. a, The main difference between the single- and many-particle equilibrium potential curve. **b**, Schemes A, B and C describe roughly the possible situation at points A, B and C in graph **a**. Although Scenario 1 is widely accepted in the literature, we show in the present article that Scenario 2 is much more likely.

fraction, thus under the constraint of equation (3). The result is

$$\mu^l = \mu^N \quad \text{for } l = 1, \ldots, N-1 \tag{4}$$

This implies that all particles must have the same chemical potential in equilibrium. Finally, the cell voltage U in the equilibrium is related to the common chemical potential $\mu = \mu^1 = \cdots = \mu^N$ of the particles by

$$U = -\frac{\mu}{e} + U_0 \tag{5}$$

where e denotes the charge of an electron and U_0 is the basic cell voltage.

The exploitation of equation (3) and the $N-1$ equation (4) give the Li mole fractions $y^1(q), y^2(q), \ldots, y^N(q)$ as functions of the total mole fraction q of the system. Next we must check whether these functions characterize equilibria. These are guaranteed by the condition that the matrix of second derivatives of the total free energy of the system is positive definite. The calculation implies that in any given state of charge, that is, for given q, this N-storage-particle system decomposes into two coexisting phases. However, one phase is represented here by all lithium-poor particles, whereas the other phase consists of all lithium-rich particles.

Selected results of models (1)–(5) are shown in Figs 3b and 5. Figure 3b shows equilibria in a system of merely 10 storage particles. Here the equilibria separate into 11 different branches. The equilibria on the same branch have the same number of storage particles in each phase. This is indicated in Fig. 3b by the pairs (n, m). For example, (8, 2) means that 8 particles have a low and 2 particles have a high Li mole fraction.

The crucial feature of the new model, however, is the prediction of processes occurring during a slow, quasi-static charge/discharge process and, indirectly, the prediction of selected phenomena occurring at the usual charge/discharge rates. We can now comment on the many-particle picture introduced descriptively in Fig. 4 (Scenario 2) in the light of the strict mathematical treatment. We start the quasi-static discharge/charge at a branch with the state (n, m), indicated in Fig. 3b, and consider a total Li fraction q that only slowly increases in time (discharging of the electrode). The process continuously evolves along that branch (n, m). If the process reaches the end of the branch, there is no further equilibrium point available on the branch (n, m). As explained above, then one particle decomposes into two phases; however, this state is not stable because the particle is a member of a many-particle ensemble. It is not stable because, in contrast to the single-particle 'thought experiment', the amount of Li in individual particles is not fixed anymore (see equation (3)). For this reason, the interface inside the particle quickly moves to establish a stable homogeneous state. During this period, the particle gathers lithium atoms from the other particles (following Scenario 2 in Fig. 4b). The ensemble now consists of $n-1$ lithium-poor particles and $m+1$ lithium-rich particles, so that the ensemble has changed to the branch $(n-1, m+1)$ of the (μ, q) plot.

In the limiting case, one could say that as we increase the total loading, we charge individual particles one-by-one rather than charge all of the particles simultaneously (as already indicated in Fig. 4b). This sequential particle-by-particle charging/discharging creates a saw-like chemical potential (or electric potential) profile if the number of particles is small (Fig. 5a). As expected, when the particle number is large, the potential smooths out (Fig. 5b, see also Fig. 4a, green line). The interconnection of particles can also be presented in terms of an equivalent circuit (see Fig. 5c,d).

© 2010 Macmillan Publishers Limited. All rights reserved.

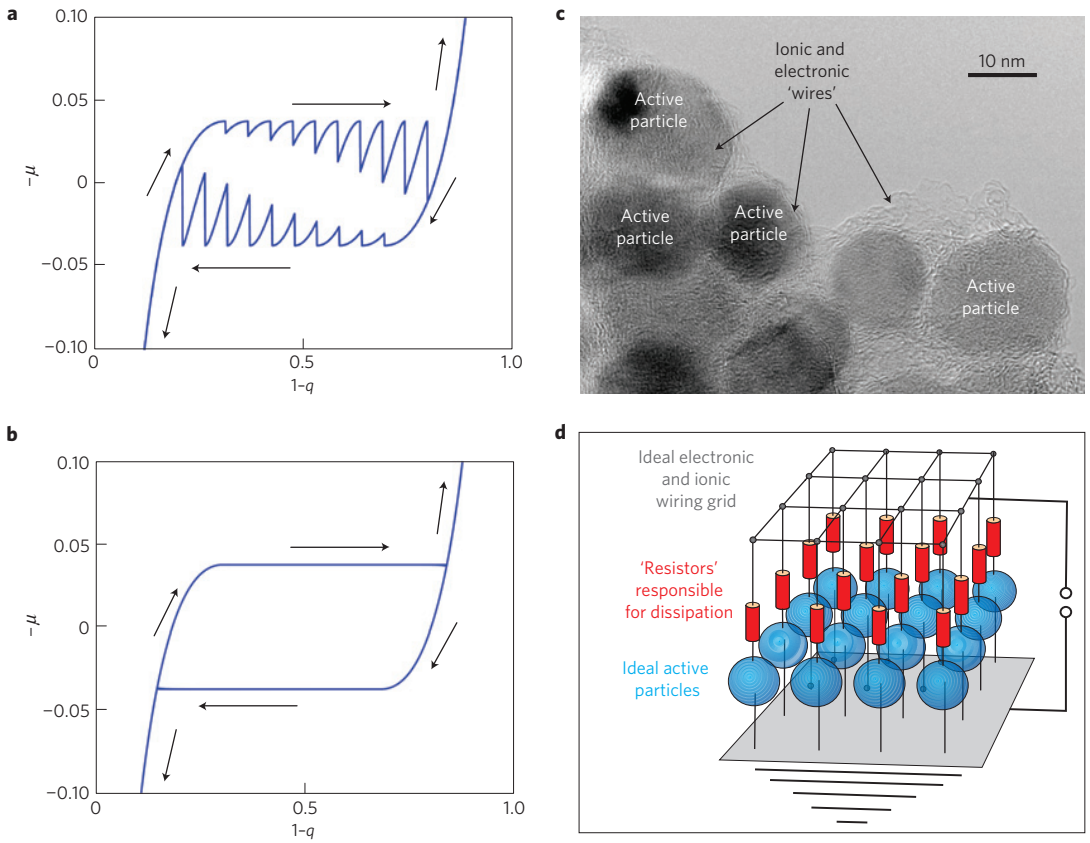

Figure 5 | Interpretation of voltage hysteresis in many-particle insertion systems with fast Li exchange between the particles and a non-monotone single-particle chemical potential. a,**b**, Simulated hysteresis loop of a full charge and discharge process for 10 (**a**) and 1,000 (**b**) particles. **c**, A typical modern cathode consisting of nanoparticulate Li_2FeTiO_4 active particles embedded into a carbon matrix (electronic conductor) and wetted by a liquid electrolyte (ionic conductor). In such cases, the requirement of fast Li exchange between the particles can occur. **d**, Equivalent circuit describing schematically the present model of hysteresis. Note that the 'resistors' are actually incorporated inside the active particles, but for clarity they are presented separately.

The prediction power of the many-particle model developed above can be demonstrated on the experiment shown before in Fig. 2d. We focus on two crucial experimental observations. The first concerns the possibility to end up in two different equilibrium states, that is, two different cell voltages within the two-phase region. Second, we observe from the experiment that one may change between the two equilibria without leaving the two-phase region. Both observations can easily be reproduced by the present many-particle model (equations (1)–(5)), as shown in Supplementary Fig. S3.

Similarly, the occurrence of hysteresis (Figs 1b–d, 2c) is a direct consequence of the fact that the many-particle system as a whole inherently contains several equilibria that lie on different branches; that is, they correspond to different phase fractions. The preferred equilibria depend on the history of the electrode.

The many-particle model is also able to explain several poorly understood phenomena reported in the battery literature. For example, the model prediction that charging/discharging proceeds sequentially (particle-by-particle) is fully supported by referring to a recent experiment by Delmas *et al.*[11], who termed this sequential process a 'domino cascade' model. Similarly, this model prediction is in excellent agreement with the finding[12] on another storage system—TiO_2 anatase. The latter work found that in nanosized TiO_2 particles there exists either only the anatase or the Li–titanate phase (the coexistence of both phases inside a given particle is not possible).

It is important to stress, once again, that the above-described hysteresis is of thermodynamic origin and will always appear in many-particle systems with a non-monotone single-particle chemical potential. Of course, this does not preclude other possible origins of hysteretic behaviour, which, however, represent only extra sources to the present one. The non-monotone single-particle behaviour is expected for most insertion battery systems. Namely, during the charge/discharge process, at least within a certain limited compositional range, most systems show a positive heat of solution, which, in a slow galvanostatic experiment, leads to a plateau-like potential profile. It is worth noting that the non-monotonicity of the chemical potential is a general phenomenon that can be observed in systems as different as pre-melted disordered crystals[13] or ordinary rubber balloons[14].

Thus, from a practical point of view, the crucial question is whether we can modify the single-particle nature in such a way that the non-monotone chemical potential will turn into a monotone one. Effectively, this would mean that we could get rid of the present source of hysteresis and thus improve the battery efficiency. Indeed, several recent experiments indicate that the nature of the chemical potential is changed from non-monotone to monotone. For example, it has been shown[15] that the two-phase nature of the $LiFePO_4/FePO_4$ system changes into a one-phase solid-solution Li_xFePO_4 system owing to the large anti-site disorder induced by the specific processing method. A similar effect has been observed[12] when the particle size of TiO_2 was decreased to the order of magnitude of 10 nm. The reasons for these phase changes are still under discussion. In the present context, however, such a change means that the occurrence of hysteresis resulting from the many-particle effect is prevented.

© 2010 Macmillan Publishers Limited. All rights reserved.

In a broader sense, the present model also offers answers to experimental results obtained at moderate or high rates. For example, unusually fast charge/discharge rates in $LiFePO_4$ nanoparticles coated with a glassy phase have recently been reported[8]. In fact, considering merely the estimated diffusion coefficient of lithium in $LiFePO_4$ of 10^{-12} cm^2 s^{-1} and assuming a particle size of 30 nm, the expected diffusional relaxation time is as short as about 10 s. This means that the corresponding charge/discharge can in principle be even significantly faster than measured in ref. 8. However, according to the present model, there is another issue besides the solid-state diffusion and the wiring effects. This extra phenomenon might lead to an unexpected scenario: below a certain critical particle size the performance will not improve anymore as the size is further reduced. This would occur as a consequence of the fact that in a multiparticle electrode the insertion does not proceed in all particles coherently (simultaneously). It could be that the sequential nature of charging/discharging has been successfully (partly) transformed into (predominantly) simultaneous charging/discharging in ref. 8. At least theoretically, such a transformation would be possible if we introduced into the system appropriate nucleation seeds for the phase transformation.

Finally, let us mention that the present many-particle model extends far beyond battery storage. It holds equally well for any system with interconnected storage particles where the individual particles show a non-monotone potential. Examples are supercapacitors, hydrogen storage particles and, last but not least, ordinary rubber balloons—if connected through a common pressure vessel. In all cases, the particles/balloons will be filled one by one forming a two-phase system, there will be multiple equilibria and there will also be a 'zero-rate' hysteresis during charge/discharge.

Methods

Li_2FeSO_4 was prepared using a published hydrothermal method reported elsewhere[16]. Briefly, the starting precursors were 0.4 mol of lithium hydroxide (Aldrich), 0.1 mol of SiO_2–Cabosil M5 (Riedel-de Haën) and 0.1 mol of Fe(II) chloride tetrahydrate (Aldrich). Fe(II) chloride solution was separately prepared under Ar and mixed with a dispersion of SiO_2 particles and LiOH. The slurry was sealed into a Teflon-lined stainless-steel autoclave and left for 15 days at 150 °C. After the hydrothermal treatment had been completed, we treated the samples with citric acid, and dried and carbonized them in a CO/CO_2 (50:50) atmosphere up to 700 °C according to different temperature regimes. TiO_2 electrodes were prepared by previous treatment of TiO_2-325 mesh (Aldrich, 248576) with a low quantity of tetraethyl orthosilicate to facilitate the ionic wiring of the TiO_2 particles[17]. TiO_2, tetraethyl orthosilicate (Aldrich, 98%), ammonia (Merck, 25%) and H_2O were mixed and the mixture kept at 40 °C in an ultrasound bath for an hour and left at 80 °C overnight to obtain a dry material. Finally, the material was thermally treated at 480 °C in an air atmosphere. $LiCoO_2$ electrodes were prepared by mixing $LiCoO_2$ (SC 20 Merck), 10 wt% of Teflon and 10 wt% of carbon black (ECP 600% JD). Ethanol was used as a solvent.

$LiFePO_4$/C composites were synthesized according to a citrate precursor method described in detail elsewhere[18]. Briefly, Fe(III) citrate (Aldrich, 22,897-4) was dissolved in water at 60 °C. Separately, an equimolar water solution of LiH_2PO_4 was prepared from H_3PO_4 (Merck 1.00573) and Li_3PO_4 (Aldrich, 33,889-3). The solutions were mixed together and the obtained transparent sol was dried at 60 °C for at least 24 h. After thorough grinding with a mortar and pestle, the obtained dried xerogel was fired in an argon atmosphere with a heating rate of 10 °C min^{-1} up to 700 °C and maintaining the final T for 10 h. This method gives porous $LiFePO_4$ particles of typical sizes between 5 and 20 μm. All particle surfaces (outer and inner) were essentially covered with a 1–2-nm-thick carbon film. The total content of native carbon was about 3 wt%.

Electrodes were prepared from the basic active material ($LiFePO_4$/C composite) to which carbon black (AE 03972, Ketjen black) and Teflon (60 wt% dispersion, Aldrich) binder were added to get a final weight ratio of 83:7:10. The obtained plastic mass was coated on an aluminium foil. Coin-type electrodes ($Ø = 16$ mm) were cut out and dried overnight at 110 °C. The conventional three-electrode cells in a coffee-bag configuration were prepared by using metallic lithium as a counter electrode and a metallic lithium strip as a reference electrode. The latter was inserted between two Celgard 2300 microporous membrane separators that divided the working and the counter electrode. The electrolyte used was a 1 M solution of $LiPF_6$ in ethylene carbonate/diethyl carbonate (1:1 ratio by volume, all received from Aldrich).

All of the electrochemical measurements were made with a PAR EG&G 283 potentiostat/galvanostat at 25.0 °C. The temperature was controlled using a thermostat (Lauda, cooling thermostat RE 212). We used a battery with an active mass of $LiFePO_4$ 9.3 mg ($Q_{theor} = 5,67$ As). Before the accurate galvanostatic measurements, we pre-cycled the electrodes at a C/10 rate. We carried out extensive galvanostatic charge/discharge cycling within the plateau voltage region with the partial charge/discharge of the tested battery (see Supplementary Information) to eliminate the edge effects of the two one-phase regions. We measured galvanostatic curves at 11 different rates extending from moderate ones (C/5) down to very low ones (C/1,000). At all of the C rates (except C/1,000), we charged/discharged 28% of the theoretical capacity of the cell. In the case of the lowest C/1,000 rate, we charged/discharged only 17% of the theoretical capacity of the battery. The partial galvanostatic cycling for each C rate was done in the following sequence: constant positive current ($+C$), relaxation, constant negative current ($-C$), relaxation. The term 'relaxation' is used for the time period during which the battery is left at the conditions of an open circuit and was typically of the order of 20–40 h.

Received 9 October 2009; accepted 23 February 2010; published online 11 April 2010

References

1. Boyanov, S. *et al. P*-redox mechanism at the origin of the high lithium storage in NiP_2-based batteries. *Chem. Mater.* **21,** 298–308 (2009).
2. Doe, R. E., Persson, K. A., Meng, Y. S. & Ceder, G. First-principles investigation of the Li–Fe–F phase diagram and equilibrium and nonequilibrium conversion reactions of iron fluorides with lithium. *Chem. Mater.* **20,** 5274–5283 (2008).
3. Ogasawara, T., Débart, A., Holzapfel, M., Novák, P. & Bruce, P. G. Rechargeable Li_2O_2 electrode for lithium batteries. *J. Am. Chem. Soc.* **128,** 1390–1393 (2006).
4. Yamada, A. *et al.* Room-temperature miscibility gap in Li_xFePO_4. *Nature Mater.* **5,** 357–360 (2006).
5. Dreyer, W., Guhlke, C. & Huth, R. The behaviour of a many particle cathode in a lithium-ion battery, WIAS Preprint No. 1423 (2009).
6. Han, B. C., Van der Ven, A., Morgan, D. & Ceder, G. Electrochemical modeling of intercalation processes with phase field models. *Electrochim. Acta* **49,** 4691–4699 (2004).
7. Amin, R., Balaya, P. & Maier, J. Anisotropy of electronic and ionic transport in $LiFePO_4$ single crystals. *Electrochem. Solid State Lett.* **10,** A13–A16 (2007).
8. Kang, B. & Ceder, G. Battery materials for ultrafast charging and discharging. *Nature* **458,** 190–193 (2009).
9. Srinivasan, V. & Newman, J. Discharge model for the lithium iron–phosphate electrode. *J. Electrochem. Soc.* **151,** A1517–A1529 (2004).
10. Srinivasan, V. & Newman, J. Existence of path-dependence in the $LiFePO_4$ electrode. *Electrochem. Solid State Lett.* **9,** A110–A114 (2006).
11. Delmas, C., Maccario, M., Croguennec, L., Le Cras, F. & Weill, F. Lithium deintercalation in $LiFePO_4$ nanoparticles via a domino-cascade model. *Nature Mater.* **7,** 665–671 (2008).
12. Wagemaker, M., Borghols, W. J. H. & Mulder, F. M. Large impact of particle size on insertion reaction. A case for anatase Li_xTiO_2. *J. Am. Chem. Soc.* **129,** 4323–4327 (2007).
13. Hainovsky, N. & Maier, J. Simple phenomenological approach to premelting and sublattice melting in Frenkel disordered ionic crystals. *Phys. Rev. B* **51,** 15789–15797 (1995).
14. Müller, I. & Strehlow, P. *Rubber and Rubber Balloons* (Lecture Notes in Physics. Vol. 637, Springer, 2004).
15. Gibot, P. *et al.* Room-temperature single-phase Li insertion/extraction in nanoscale Li_xFePO_4. *Nature Mater.* **7,** 741–747 (2008).
16. Dominko, R., Conte, R. D., Hanzel, D., Gaberscek, M. & Jamnik, J. Impact of synthesis conditions on the structure and performance of Li_2FeSiO_4. *J. Power Sources* **178,** 842–847 (2008).
17. Erjavec, B. *et al.* Tailoring nanostructured TiO_2 for high power Li-ion batteries. *J. Power Sources* **189,** 869–874 (2009).
18. Dominko, R. *et al.* Wired porous cathode materials: A novel concept for synthesis of $LiFePO_4$. *Chem. Mater.* **19,** 2960–2969 (2007).

Acknowledgements

The main idea for this work was developed within the former ALISTORE Network of Excellence (now ALISTORE-ERI). The work has been partly supported by the Slovenian Research Agency (Grant No. P2-0148). Another part of the work was carried out as part of Project C26 'Storage of Hydrogen in Hydrides' of the DFG research centre MATHEON, Berlin.

Author contributions

All authors contributed equally to this manuscript.

Additional information

The authors declare no competing financial interests. Supplementary information accompanies this paper on www.nature.com/naturematerials. Reprints and permissions information is available online at http://npg.nature.com/reprintsandpermissions. Correspondence and requests for materials should be addressed to M.G.

© 2010 Macmillan Publishers Limited. All rights reserved.